Alternative Splicing Determines the Binding of Platelet-Derived Growth Factor (PDGF-AA) to Glycosaminoglycans †

ARTICLE *in* BIOCHEMISTRY · OCTOBER 1996

Impact Factor: 3.02 · DOI: 10.1021/bi960118l · Source: PubMed

Alternative Splicing Determines the Binding of Platelet-Derived Growth Factor (PDGF-AA) to Glycosaminoglycans†

Florentyna Lustig,*,‡ Johan Hoebeke,‖ Gunnel Östergren-Lundèn,‡ Florence Velge-Roussel,‖ Göran Bondjers,‡ Urban Olsson,‡ Ulla Rüetschi,§ and Gunnar Fager‡

The Wallenberg Laboratory for Cardiovascular Research, Sahlgrenska University Hospital, S-413 45 Göteborg, Sweden, The Department of Clinical Chemistry, University of Göteborg and Sahlgren's Hospital, S-400 33 Göteborg, Sweden, and CJF93/09 INSERM, Faculte des Sciences Pharmaceutiques, Université Francois Rabelais, F-37200 Tours Cedex, France

Received January 18, 1996; Revised Manuscript Received July 2, 1996⊗

ABSTRACT: We have shown previously that the platelet-derived growth factor (PDGF) and a synthetic oligopeptide, corresponding to the basic carboxyl-terminal amino acid extension of the long PDGF-A isoform, bind to heparin. Here, we have expressed the long (rA_{125}) and the short (rA_{109}) variants of PDGF A-chains in *Escherichia coli* and produced the functional homodimers. Surface plasmon resonance analyses showed that while the dimeric rA_{125} bound with high affinity to low molecular weight heparin, the rA_{109}, lacking the basic extension, did not. This strongly indicated that high affinity binding is due to the carboxyl-terminal extension. Investigations of kinetics and thermodynamics suggested an allosteric binding mechanism. Thus, dimeric rA_{125} contains two equivalent binding sites. Following low affinity binding of heparin to one binding site, the dimer undergoes a conformational change, increasing the affinity for heparin about 40 times. This positive cooperativity requires the basic amino acid extension in both monomers of the dimeric PDGF molecule. Thermodynamics of the reaction, showing an entropy-driven endothermic process, suggest the involvement of hydrophobic interactions in this rearrangement. Three amino acids in the basic carboxyl-terminal extension were essential for the interaction: the basic residues Arg^{111} and Lys^{116}, and the polar Thr^{125}. We also found that other glycosaminoglycan species, corresponding to those produced by human arterial smooth muscle cells, bound to dimeric rA_{125} and that heparan sulfate showed the highest affinity.

The accumulation of smooth muscle cells (SMCs)[1] in the arterial intima is a well-recognized feature of atherosclerosis, especially prominent in transplant atherosclerosis and restenosis after balloon angioplasty or coronary bypass grafting (Ross et al., 1990). The increase in arterial SMC (ASMC) mass is due to migration from the media as well as proliferation within the intima/media and has been associated with activity of the platelet-derived growth factor (PDGF) (Ross, 1981; Schwartz et al., 1986; Thyberg et al., 1990). However, the proliferation of these cells is also under the influence of several other cytokines including fibroblast growth factors (FGFs) (Lindner & Reidy, 1991), interleukins, and α-thrombin (Bobik & Campbell, 1993; Fager, 1995).

PDGF is a disulfide-linked dimer composed of two polypeptide chains, denoted A and B and represented *in vivo* by all three chimeras; PDGF-AA, PDGF-AB, and PDGF-BB (Heldin et al., 1986; Hart et al., 1990). There are two isoforms of the PDGF-A chain. This is a result of translation of two PDGF A-chain transcripts, arising from alternative usage of exon 6 coding for a basic amino acid sequence. Thus, only the longer A-chain isoform contains a sequence with a high proportion of lysine and arginine residues in its carboxyl-terminal extension.

The conservation of A- and B-chains of PDGF can be associated with the existence of distinct α and β cell-surface PDGF receptors and their recognition pattern. Several attempts have been made to explain the biological role of the carboxyl-terminal extension of the long A-chain. According to Maher et al. (1989), this basic sequence is responsible for targeting a nonsecreted form of the A-chain to the nucleus. On the other hand, increasing evidence suggests an involvement of the basic carboxyl-terminal in binding of PDGF to glycosaminoglycans (GAGs) (Fager et al., 1992a,b; Raines & Ross, 1992; Khachigian & Chesterman, 1992). Heparin-like GAGs bind PDGF and inhibit its mitogenic effect on human ASMC (hASMC) *in vitro* (Fager et al., 1992a). An oligopeptide (Oligo-108−124), corresponding to the exon 6-derived amino acid residues 108−124 of the long PDGF A-chain isoform, bound to heparin−Sepharose and competed with PDGF for binding to heparin. By interfering with the binding of PDGF to heparin, the

† This study was supported by grants from the Swedish Medical Research Council (Project No. 4531) and the Swedish Heart Lung Foundation (Project No. 51044).

* Author to whom correspondence should be addressed.

‡ The Wallenberg Laboratory for Cardiovascular Research, University of Göteborg, Sweden.

§ The Department of Clinical Chemistry, University of Göteborg, Sweden.

‖ Faculte des Sciences Pharmaceutiques, Université Francois Rabelais, Tours Cedex, France.

⊗ Abstract published in *Advance ACS Abstracts,* August 15, 1996.

[1] Abbreviations: PDGF, platelet-derived growth factor; rA_{109}, short recombinant PDGF A-chain; rA_{125}, long recombinant PDGF A-chain; nA_{125}, native PDGF A-chain; aFGF, acidic fibroblast growth factor; bFGF, basic fibroblast growth factor; AT-III, antithrombin III; SMC, smooth muscle cells; hASMC, human arterial smooth muscle cells; LMW-heparin, low molecular weight heparin (M_r = 3000); GAG(s), glycosaminoglycan(s); PG(s), proteoglycan(s); HS, heparan sulfate; DS, dermatan sulfate; CS, chondroitin sulfate; UF, unretained fraction obtained after subfractionation of fresh human serum on heparin−Sepharose column; LDL, low density lipoproteins; PMSF, phenylmethanesulfonyl fluoride; Gdn-HCl, guanidine hydrochloride; BSA, bovine serum albumin; SPR, surface plasmon resonance.

S0006-2960(96)00118-3 CCC: $12.00

oligopeptide relieved the block on hASMC proliferation induced by heparin *in vitro*. According to our later results, the hASMC-derived heparan sulfate (HS), dermatan sulfate (DS), and chondroitin sulfate (CS) species also bound PDGF A-chains via this sequence (Fager et al., 1995). We further found that binding to HS, DS, and heparin inhibited the mitogenic properties of PDGF.

In this work we wanted to directly evaluate the binding of dimeric rA_{109} and rA_{125} to heparin, in a simplified *in vitro* system. Heparin was selected as a well characterized commonly used reference GAG. We also wanted to identify the particular amino acids essential for this binding using synthetic oligopeptides with different amino acid substitutions. Since binding and inactivation of PDGF by heparin may not reflect the *in vivo* situation where different GAGs are present, we also investigated if other GAG species interacted with PDGF-AA.

EXPERIMENTAL PROCEDURES

Materials. All chemicals were of highest available purity. Plasmid BBG 31 containing cDNA for the long PDGF-A chain isoform, rPDGF-AA (dimeric $rA_{126(R\&D)}$), PDGF-AB, and aFGF were obtained from R&D Systems (Abingdon, U.K.). The expression vector pET-3a and *Escherichia coli* BL21(DE3)pLysS cells were generously provided by Dr. F. W. Studier (Brookhaven National Laboratory, Upton, NY). Bacterial growth media were from Kebo (Göteborg, Sweden). [6-^{3}H]Thymidine was from Amersham (Buckinghamshire, U.K.) and heparin sodium pure (powder) from porcine intestinal mucosa was from Leo Pharmaceutical Products (Ballerup, Denmark). Low molecular weight (LMW) heparin (average $M_r = 3000$) was obtained from Sigma Chemical Co. (St. Louis, MO). Heparan sulfate (from bovine kidney, Cat. No. 400700), chondroitin sulfate C (from shark cartilage, Cat. No. 400675), and dermatan sulfate (chondroitin sulfate B from pig skin, Cat. No. 400660) were from Seikagaku Corp. (Tokyo, Japan). Cell culture media were from Flow Laboratories (Irvine, Scotland). Human blood serum was from young healthy donors. Oligonucleotides were synthesized using a Model 381A DNA synthesizer (Applied Biosystems, Foster City, CA) essentially as recommended by the manufacturer. Chemicals used for synthesis were either from Applied Biosystems or from Perkin-Elmer Cetus, Norwalk, CT.

Cloning and Expression of the PDGF A-Chains in E. coli. The cDNA for the long PDGF-A chain (containing exon 6), cloned between the *Hin*dIII and *Bam*HI in the polylinker of pUC18 (plasmid BBG 31), codes for a 126 amino acids long A-chain ($rA_{126(R\&D)}$) with the basic extension in its carboxyl-terminus (Table 1). The gene contains a *Pst*I site approximately 30 nucleotides downstream from the 5'-terminal *Hin*dIII site. A *Pst*I−*Bam*HI fragment (360 bp) was cut out and purified on low melting point agarose. An *Nde*I−*Pst*I fragment corresponding to the 5'-end of the gene (obtained by annealing of two complementary synthetic oligonucleotides 5′-TAT GAT CGA GGA AGC TGT CCC TGC A-3′ and 5′-GGG ACA GCT TCC TCG ATC A-3′) was ligated to the *Pst*I−*Bam*HI fragment. The resulting *Nde*I−*Bam*HI fragment (384 bp), corresponding to the gene for the long PDGF-A chain but lacking its own promoter, was cloned into the expression vector pET-3a under the T7 promoter. The final construct, designed pET-3a/PDGF-A_{125}, coded for the long rPDGF-A chain (rA_{125}).

Table 1: Carboxyl-Terminal Amino Acid Sequences of Native and Recombinant PDGF A-Chain Variants[a]

residue no.	nA_{125} rA_{125}	nA_{110}	rA_{109}
104	Glu	Glu	Glu
105	Glu	Glu	Glu
106	Asp	Asp	Asp
107	Thr	Thr	Thr
108	Gly	Asp	Gly
109	Arg	Val	Arg
110	Pro	Arg	COOH
111	Arg	COOH	
112	Glu		
113	Ser		
114	Gly		
115	Lys		
116	Lys		
117	Arg		
118	Lys		
119	Arg		
120	Lys		
121	Arg		
122	Leu		
123	Lys		
124	Pro		
125	Thr		
	COOH		

[a] The rPDGF-A isoforms were produced as described under Experimental Procedures; nA, native, and rA, recombinant PDGF A-chain.

The gene for the short PDGF-A chain (rA_{109}) was constructed as follows. The cDNA for the long PDGF-A chain contains a *Stu*I site at position 345 in front of the exon 6 sequence. The pET-3a/PDGF-A_{125} was digested with restriction enzymes *Stu*I/*Bam*HI and ligated with a *Stu*I−*Bam*HI fragment containing three stop codons. This fragment was derived from annealing of complementary synthetic oligonucleotides 5′-TGA TAA TAA CCC GG-3′ and 5′-GAT CCC GGG TTA TTA TCA-3′. In this way, we obtained the pET-3a/PDGF-A_{109} coding for the shorter A-chain consisting of 109 amino acids (rA_{109}) and lacking the basic sequence corresponding to exon 6.

Table 1 shows the carboxyl-terminal sequences of the native A-chains and A-chains coded by the two gene constructs. Both long isoforms, rA_{125} and native A_{125} (nA_{125}), are identical in their carboxyl-terminal amino acid sequences. The short rA_{109} variant differs slightly from the native short A-chain (nA_{110}) in its carboxyl-terminal sequence. In the amino-terminus of rA constructs, a methionine replaced the terminal serine of the native variants. The recombinant pET-3a vectors (pET-3a/PDGF-A_{125} and pET-3a/PDGF-A_{109}) were used for transformation of *E. coli* BL21(DE3)pLysS cells carrying the inducible gene for T7 RNA polymerase. The transformants were further grown and the synthesis of PDGF was induced according to Elias et al. (1990).

Preparation of Monomeric rA_{125} and Monomeric rA_{109}. The *E. coli* cells were harvested and lysed (Elias et al., 1990) and PDGF-A monomers prepared essentially as described (Hoppe et al., 1989). Briefly, the lysate was centrifuged for 30 min at 25000*g*. The pellet with inclusion bodies, containing about 90% of the overexpressed A-chain, was dissolved in 10 mL of 50 mM Tris-HCl, 2% SDS, 2% mercaptoethanol, 2 mM benzamidine, and 0.1 mM PMSF, pH 7.8, and shaken for 1 h at 37 °C. The sample was precipitated with acetone and centrifuged, and the precipitate dissolved in 5 mL of 4 M guanidine hydrochloride (Gdn-

Table 2: Synthetic Oligopeptide Variants Used in Displacement Experiments

amino acid residue	Oligo							
	RKT	AKT	RAT	RKA	AAT	AKA	RAA	AAA
111	Arg	Ala	Arg	Arg	Ala	Ala	Arg	Ala
116	Lys	Lys	Ala	Lys	Ala	Lys	Ala	Ala
125	Thr	Thr	Thr	Ala	Thr	Ala	Ala	Ala

HCl), 2 mM benzamidine, and 0.1 mM PMSF. After dialysis against 3 × 5 L of H_2O the monomers were concentrated in vacuo. The dried material was further dissolved in 1 M acetic acid, and the monomers were purified on a P10 (Bio-Rad) column (1.6 × 90 cm) using 1 M acetic acid (pH adjusted to 3.5 with NH_4OH) for elution. The fractions containing the monomers were combined and dried in vacuo. The recombinant monomers obtained in this way (denoted monomeric rA_{125} and monomeric rA_{109}) were dissolved in 1 M acetic acid and stored at 20 °C.

Purification of Recombinant PDGF-A Monomers. The monomers were obtained as described above. The acetone precipitate was dissolved in 5 mL of 4 M Gdn-HCl, 2 mM benzamidine, and 0.1 mM PMSF, and pH was raised to 7.5 by the addition of concentrated NaOH solution.

Thiol groups were protected by S-sulfonation (Hope et al., 1989). The S-sulfonated rPDGF-A monomer was purified on a Sephacryl S200 (Pharmacia, Uppsala, Sweden) column (2.6 × 55 cm) by elution with 4 M Gdn-HCl, 50 mM Tris-HCl, 2 mM benzamidine, and 0.1 mM PMSF, pH 7.8. Aliquots of fractions were analyzed by 8−25% SDS−PAGE (Phast System, Pharmacia, Uppsala, Sweden). Fractions containing the recombinant monomer were pooled, dialyzed against 3 × 5 L of H_2O, and concentrated either by acetone precipitation or in vacuo.

Dimerization of rPDGF-A Monomers and Purification of Dimers. Recombinant PDGF-A monomers were dimerized in the presence of glutathione (Hoppe et al., 1989) for 2−3 days at 20 °C. Dimerization occurred with 20−50% efficiency.

The preparation was precipitated with 4 volumes of acetone and the recovered pellet dissolved in 1 M acetic acid. Dimers and monomers were separated on a P10 column as described above. The fractions were tested by SDS−PAGE as above. Fractions containing the dimers were pooled and concentrated in vacuo. The recombinant homodimers were dissolved in 1 M acetic acid and stored at −20 °C. In this way, we obtained homodimers of rA_{125} and rA_{109} denoted dimeric rA_{125} and dimeric rA_{109}, respectively.

Total protein was assessed by the Bio-Rad protein assay (Bio-Rad Laboratories, Richmond, CA) with BSA as standard. The peptide concentrations were confirmed by amino acid analysis of the total hydrolysates of the peptides.

Preparation of Synthetic Oligopeptides. Oligopeptides were synthesized utilizing F-moc temporary α-amino protection in a MilliGen 9050 Pepsyntheziser according to the manufacturer (Millipore, Bedford, MA) as previously described (Fager et al., 1992b). Oligo-RKT corresponded to the carboxyl-terminal amino acids 108−125 of the long PDGF A-chain isoform (Tables 1 and 2). Substitutions for alanine at positions Arg^{111}, Lys^{116}, and Thr^{125} yielded another oligopeptide, Oligo-AAA. All possible mono- and disubstituted variants of this peptide were also prepared (Table 2). The correct amino acid sequences were confirmed and peptide concentrations determined as described (Fager et al., 1992b).

Cell Culture Experiments. Experiments with hASMC were carried out essentially as described previously (Fager et al., 1992a,b) according to details described in legend to Figure 1.

Surface Plasmon Resonance (SPR) Analyses. All measurements were performed with a BIAcore system (Pharmacia Biosensor) and CM5 sensor chips essentially as described by Mach et al. (1993). This technique monitors the real-time binding of protein molecules to a ligand immobilized on the dextran-derivatized sensor chip surface. In these experiments biotinylated low molecular weight (LMW) heparin was immobilized on streptavidin covalently bound to the chip matrix. Binding of protein ligands was measured as refractive index changes (given in resonance units, RU), which directly correlated with the amount of protein bound to the surface.

Immobilization of LMW-Heparin on BIAcore Sensor Chips. The surface of a sensor chip CM5 was activated by injecting 8 μL of a mixture of 0.2 M *N*-ethyl-*N*′-((diethylamino)propyl)carbodiimide (EDC) and 0.05 M *N*-hydroxysuccimide (NHS) (Pharmacia Biosensor). Before immobilization of streptavidin, the surface was equilibrated with the running buffer (PBS buffer, containing 5 mM Na_2SO_4, 1 mM EDTA, and 0.05% Tween 20, pH 7.2) at a flow rate of 5 μL/min. Then, 30 μL of streptavidin (Sigma, 100 μg/mL in 10 mM sodium acetate, pH 4.5) was injected (5 μL/min) followed by injection of 1 M ethanolamine hydrochloride, pH 8.5. Oxidation of LMW-heparin (4.5 mg/mL) was performed at room temperature in 0.1 M sodium acetate, pH 5.5, containing 3.3 mM sodium metaperiodate. After a 1 h incubation, the oxidation was stopped by adding an excess of sodium sulfite. The LMW-heparin was further incubated with a 6-fold molar excess of biotinyl-LC-hydrazine (Calbiochem-Novabiochem Corp., San Diego, CA, USA) for 1 h. The excess biotin was then removed on a PD10 column (Pharmacia). Thirty microliters of biotinylated LMW-heparin (3 g/L) was injected at a flow rate of 5 μL/min into the biosensor channel and the channel washed extensively with running buffer.

Determination of Binding Affinity and Kinetics of Proteins and Peptides to LMW-Heparin. The experiments were run at indicated temperatures (Table 3). Stock solution of dimeric rA (20 mg/mL) was diluted in running buffer to indicated concentrations and injected into the Biosensor cell at a flow rate of 2 μL/min. After each experiment, the heparinized biosensor surface was regenerated with 10 μL of 0.1 M NaOH followed by 10 μL of biotinylated LMW-heparin and extensive washing with running buffer. Kinetics analyses were performed using a double exponential analysis of the association curves as described elsewhere (Velge-Roussel et al.,1995).

The biosensor cell was perfused at 30 °C with a mixture of dimeric rA_{125} and synthetic oligopeptides in indicated concentrations (cf. Figure 6). This allowed further evaluation of the importance of different amino acids in the basic carboxyl-terminal extension of the long PDGF-A chain for binding to heparin.

The displacement of dimeric rA_{125} from immobilized LMW-heparin by other GAG species was studied at 30 °C by perfusing the biosensor with a mixture of recombinant

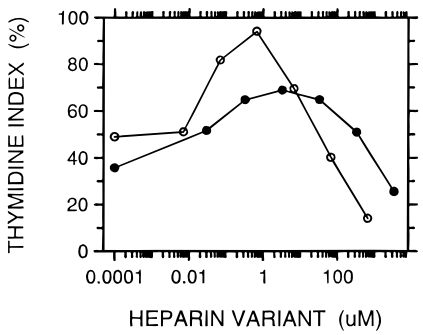

FIGURE 1: Dose-dependent inhibition of thymidine incorporation in hASMC in human serum by standard heparin and LMW-heparin. Human ASMC (approximately 500 cells/cm^2) were allowed to establish in S-BM (supplemented Waymouth's medium MB 752/1 (Fager et al., 1988,1989) with 10% human serum) in 8-chamber slides for 3 days and were then growth arrested in serum-free medium for 4 days. The cultures were further growth-stimulated in 10% human serum with indicated concentrations of standard (○−○) and LMW (●−●) heparin. Thymidine indices are given as percent of control cultures grown in 10% human serum (mean value of triplicate wells).

material (400 nM) and indicated concentrations of GAGs (cf. Figure 7).

RESULTS

Characterization of Recombinant A_{125} and A_{109}. The correct properties of the rA produced in the above system were confirmed by several methods. The dimerized rA_{125} and rA_{109} proteins showed an expected mobility compared to the PDGF-AA obtained from R&D Systems (dimeric $rA_{126(R\&D)}$) on 8−25% SDS−PAGE (data not shown).

The correct carboxyl-terminal sequences of rA_{125} and rA_{109} were confirmed by amino acid sequencing. The peptide was first cleaved at Asp^{106} with endoproteinase Asp-N (Boehringer Mannheim GmbH, Germany), which specifically cleaves peptide bonds amino-terminally to aspartic acid. The carboxyl-terminal peptide, obtained in this way, was further sequenced by Edman degradation using an Applied Biosystems 477A protein sequencer (Foster City, CA).

Both homodimers, dimeric rA_{125} and rA $_{109}$, were biologically active and stimulated thymidine index in cultured hASMC to approximately 30% of control stimulation with 10% human serum (data not shown).

Taken together, these experiments indicated that both recombinant PDGF-A homodimers had the correct molecular and biological properties.

Comparison between Standard and LMW-Heparins on DNA Synthesis in Cultured hASMC. The growth inhibitory capacities of heparin and LMW-heparin were compared as thymidine index in human ASMC grown in medium with 10% human serum after addition of different concentrations of the heparins. Both heparin variants almost completely (80−90%) inhibited [^{3}H]thymidine incorporation into DNA at concentrations of 10 mg/mL (Figure 1).

The 50% inhibitory concentration (IC_{50}) for standard heparin was approximately 0.04 mM, while that of LMW-heparin was about 2 mM, suggesting that standard heparin (M_r 10 000−30 000 approximately) is a better inhibitor than LMW-heparin (M_r = 3,000). The LMW-heparin (Sigma), prepared by free-radical induced cleavage of standard heparin and size fractionation of the products, contains a mixture of oligosaccharides with the average M_r of 3000. Thus,

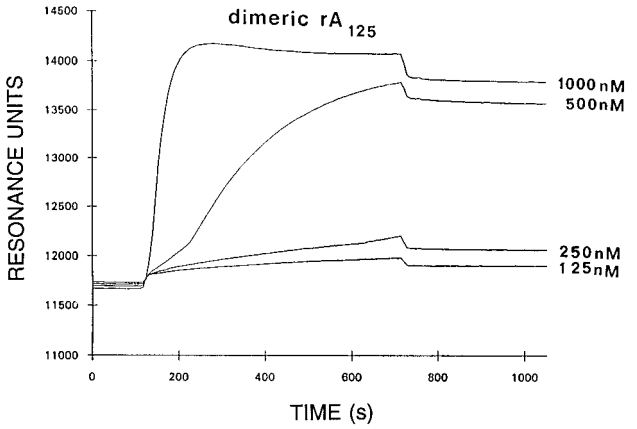

FIGURE 2: Surface plasmon resonance sensogram of the association and dissociation of dimeric rA_{125} to a heparinized biosensor surface. Indicated concentrations of dimeric rA_{125} were injected over the heparinized biosensor. The amount of protein associating/dissociating from the surface over time was measured in resonance units (RU) as described in Experimental Procedures.

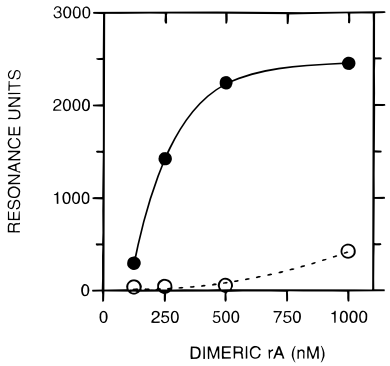

FIGURE 3: Comparison between the binding of dimeric rA_{125} and rA_{109} to immobilized LMW-heparin at surface plasmon resonance analysis. The RU values at equilibrium were calculated as described under Experimental Procedures. The resonance units presented in the y-axis correspond to RU_{max} calculated according to Velge-Roussel et al. (1995). Binding of dimeric rA_{125} (●−●) and rA_{109} (○−○) to LMW-heparin at 26 °C.

probably only some of these oligosaccharides may carry intact binding sites for PDGF. This could be at least partly the reason for the lower molar inhibitory capacity of LMW-heparin compared to standard heparin. In further experiments the LMW-heparin was used as a homogenous size substitute for the heterogenous standard heparin in kinetic binding experiments to facilitate evaluation of molar binding kinetics.

Evaluation of Interaction of Dimeric rA_{125} and rA_{109} with Immobilized LMW-Heparin by Surface Plasmon Resonance Analysis. Using LMW-heparin as the immobilized phase on the Biosensor chip, the kinetics and the thermodynamics of the interaction with dimeric rA_{125} or rA_{109} were studied. SPR sensograms of the association and dissociation of dimeric rA_{125} to the biosensor surface over time are shown in resonance units (RU) in Figure 2. These curves suggest a high affinity binding of dimeric rA_{125}. In contrast, SPR experiments with dimeric rA_{109} resulted in a very low increase in RU values (10−20% of that of the dimeric rA_{125}) even at 1 μM concentration (Figure 3). This suggests a very low affinity. In order to exclude the possibility of nonspecific adsorption, the binding of dimeric rA_{109} to the chip with immobilized streptavidin without biotinylated LMW-heparin was tested. This experiment did not show any increase in

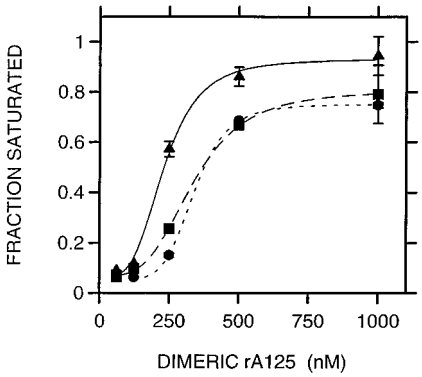

FIGURE 4: Equilibrium binding of dimeric rA_{125} at different temperatures at surface plasmon resonance analysis. The amount of binding was calculated from the sensograms as indicated under Experimental Procedures. The maximal binding was calculated by a Multifit program using the Hill plot, and the binding values were expressed as fractions of maximal binding. The S-shape of the curves indicates a positive cooperativity. The endothermicity of the complex formation at 36 °C (▲−▲) , 31 °C (■−■), and 26 °C (●−●) is indicated by the leftward shift of the curves with increasing temperatures.

Table 3: Thermodynamic Parameters of Dimeric rA_{125}, PDGF-AB, Monomeric rA_{125}, and aFGF Interaction with LMW-Heparin[a]

protein/peptide	t, °C	K_D, μM (overall)	n (Hill coeff)	$-\Delta F$,[b] kJ/mol	ΔH,[b] kJ/mol	ΔS,[b] J/(mol·K)
dimeric rA_{125}	26	0.50	2.0	36.1		
	31	0.41	1.6	37.1	+59	+329
	37	0.23	2.1	39.3		
PDGF-AB	25	0.10	1			
monomeric rA_{125}	25	≥6[c]	1			
aFGF	25	0.39	1			

[a] The dissociation constants (K_D) and the Hill coefficients (n) were calculated from the values shown in Figure 5 by a Multifit program using the Hill plot $\{\ln(F/1 - F)$ against $[rA_{125}]\}$ in which F is the fraction bound. The enthalpy changes (ΔH) and entropy changes (ΔS) were calculated by plotting the free energy change (ΔF) as a function of the absolute temperature. [b] ΔH and ΔS of the reaction were calculated from $\Delta F = -Rt \ln(1/K_D) = \Delta H - T\Delta S$. [c] Data extrapolated from Scatchard plot (highest concentration used 1 μM).

RU. Thus, the observed increase in RU at a 1 μM concentration of dimeric rA_{109}, in the presence of LMW-heparin (Figure 3), was due to low affinity binding to heparin and not to nonspecific adsorption on the chip.

In the case of dimeric rA_{125}, the S-shaped kinetic curve (Figure 2) implied a complex binding mechanism. This was confirmed by the equilibrium studies performed at different concentrations of dimeric rA_{125}, which showed binding isotherms that had a sigmoid shape (Figure 4). This suggested a positive cooperativity of the interaction. Analysis of the Hill plot gave a Hill coefficient of 1.6−2.1 for the dimeric rPDGF-A_{125}, depending on temperature (Table 3). These results were consistent with a Monod−Wyman−Changeux allosteric model (Monod et al., 1965). According to this model, a low affinity binding dimeric conformer changes to a high affinity binding conformer after a first weak binding at one of the sites.

The Hill plot also allowed the determination of the overall dissociation constant (K_D) of the heparin−PDGF interaction at different temperatures. From these results the changes of the thermodynamic parameters of the complex could be calculated. As seen in Table 3, the interaction of LMW-heparin with dimeric rA_{125} is an entropy-driven [$\Delta S = 329$ J/(mol·K)] endothermic ($\Delta H = 59$ kJ/mol) process. The magnitude of the thermodynamic parameter changes could be explained by the conformational changes inherent to a positive cooperativity model. The positive enthalpy and entropy changes suggest that hydrophobic interactions are involved.

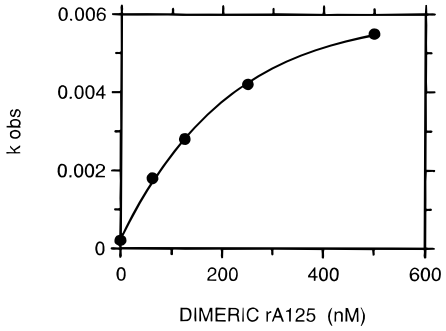

FIGURE 5: Diagram representing the association kinetics of binding of dimeric rA_{125} to immobilized LMW-heparin at surface plasmon resonance analysis. The association constants (31 °C) observed at different concentrations of dimeric rA_{125} were calculated as described under Velge-Roussel et al. (1995). The results are shown in Table 3. The obtained parable was analyzed as two step reaction in which the first one is the low affinity binding step and the second the isomerization step leading to high affinity interaction (Hoebeke et al., 1987).

Further analysis of the observed association rate constants (k_{obs}) showed a hyperbolic concentration dependency for dimeric rA_{125} (Figure 5). This observation is in accordance with the Monod−Wyman−Changeux model and confirms a two step binding mechanism: first, a weak bimolecular interaction between heparin and dimeric rA_{125}, and second, an isomerization to a high affinity conformer (Hoebeke et al., 1987) according to the following reaction:

$$A + H \underset{}{\overset{K_1}{\Longleftrightarrow}} AH \underset{k_{-2}}{\overset{k_2}{\Longleftrightarrow}} AH^*$$

where A denotes dimeric rA_{125}; H, LMW-heparin; AH, low affinity complex; and AH*, the high affinity complex.

A kinetic analysis was based on the following equation:

$$k_{obs} = (k_2K_1[A]/1 + K_1[A]) + k_{-2}$$

in which k_{obs} (s^{-1}) is the measured association rate constant, K_1 (M^{-1}) is the equilibrium constant of the binding step, k_2 (s^{-1}) is the forward rate constant of the isomerization step, k_{-2} (s^{-1}) is the reverse rate constant of the isomerization step, and $K_2 = k_2/k_{-2}$ is the equilibrium constant of the isomerization step.

The affinity constant regulating the first step is in accordance with the overall affinity constant calculated from the equilibrium studies, which should be half of the constant calculated from the kinetic data. The calculated kinetic constants were as follows: $K_1 = 4.0 \times 10^6\ M^{-1}$, $k_2 = 8.0 \times 10^{-3}\ s^{-1}$, $k_{-2} = 1.9 \times 10^{-4}\ s^{-1}$.

Thus, the ratio between the kinetic constants of the isomerization step (k_2/k_{-2}) gives an equilibrium between the high and low affinity conformers (K_2) of 42, suggesting that less than 2.5% of the heparin-dimeric rA_{125} complex is in the low affinity conformation. This is also consistent with the Monod−Wyman−Changeux conformational model. The

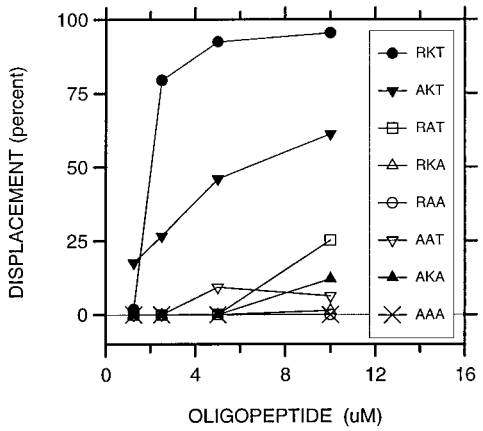

FIGURE 6: Inhibition of binding of dimeric rA_{125} to immobilized LMW-heparin by synthetic oligopeptides at surface plasmon resonance analysis. The mixture of dimeric rA_{125} (400 nM) and synthetic oligopeptides, in indicated concentrations, was perfused into the biosensor and the inhibition of binding of rA_{125} to immobilized LMW-heparin measured by surface plasmon resonance analysis. The symbols denoting different oligopeptides are indicated in the figure. The RU values at equilibrium were calculated as described under Experimental Procedures and the results expressed as % inhibition compared to the binding of dimeric rA_{125} in the absence of added oligopeptides.

real high affinity constant, being the product of the equilibrium constants of the two steps ($K_1 \times K_2$), is thus 1.7×10^8 M^{-1}.

As mentioned before, the only structural difference between the dimeric rA_{125} and rA_{109} is the basic carboxyl-terminal extension of the long PDGF variant. In order to see if the basic sequence is the only prerequisite of cooperativity and high affinity binding, we tested the binding characteristics of monomeric rA_{125} in SPR (Table 3). Although this monomer binds to LMW-heparin with low affinity ($K_D = 6.2$ μM), the interaction does not show any cooperativity. Similarly, the binding of aFGF to LMW-heparin showed that although this monomeric growth factor binds with an affinity ($K_D = 0.39$ μM) similar to the overall affinity of dimeric rA_{125}, no conformational change was observed (Hill coeff = 1). Experiments with dimeric PDGF-AB, containing the long A-chain and a B-chain, showed a monophasic binding curve with a Hill coeff of 1 and K_D of 0.1 μM. Thus, our results imply that the basic amino acid extension in both monomers of the dimeric PDGF molecule is required for the cooperative binding, which leads to the high affinity of dimeric rA_{125} to LMW-heparin.

Identification of Specific Amino Acids in the Basic Carboxyl-Terminal Extension of Dimeric rA_{125}, Required for High Affinity Binding to LMW-Heparin. Based on the striking differences between dimeric rA_{125} and rA_{109}, the high affinity binding to heparin can be ascribed to the basic carboxyl-terminal extension of the long A-chain isoform. This conclusion was further supported by the experiments with synthetic oligopeptides containing amino acid substitutions denoted in Table 2. The oligopeptide derived from the carboxyl-terminal sequence (Oligo-RKT) efficiently inhibited ($IC_{50} = 2$ μM) binding of dimeric rA_{125} to LMW-heparin at SPR analysis (Figure 6). Consequently, we wanted to identify the amino acids in Oligo-RKT essential for the interaction with LMW-heparin. Based on earlier results, it was assumed that lysine residue 115 and/or 116 should be among the relevant residues for binding to heparin (Fager et al., 1992b, 1995). Recently, Thompson et al.

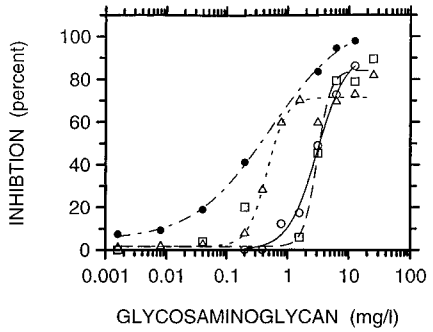

FIGURE 7: Measurement of inhibition of binding of dimeric rA_{125} to immobilized LMW-heparin by different GAG species at surface plasmon resonance analysis. Dimeric rA_{125} (400 nM) was preincubated with indicated concentrations of LMW-heparin (●−●), HS (△−△), DS (□−□), and CS (○−○) and allowed to interact with the immobilized LMW-heparin in the biosensor chamber. The RU values at equilibrium were calculated as described under Experimental Procedures and the results expressed as % inhibition compared to the binding of dimeric rA_{125} in the absence of added glycosaminoglycans. The experiments were run at 30 °C.

(1994) reported three amino acids in the basic sequence of bFGF to be important for binding to heparin, namely, Arg^{120}, Lys^{125}, and Gln^{134}. By comparing the heparin-binding motif of rA_{125} with the corresponding motif of bFGF (Table 4), three commonly positioned types of amino acids were identified, Arg^{111}, Lys^{116}, and Thr^{125}. Substitutions for alanine at these positions yielded an oligopeptide, Oligo-AAA (Table 2), which did not inhibit the binding of dimeric rA_{125} to LMW-heparin (Figure 6). These results show that essentially three specific amino acids account for the high affinity interaction between heparin and dimeric rA_{125}. Among these amino acids, oligopeptides carrying the Thr^{125} to Ala^{125} substitution were least efficient in displacing dimeric rA_{125} from binding to immobilized LMW-heparin followed by substitutions of the Lys^{116} to Ala^{116} and Arg^{111} to Ala^{111} residues in falling order of importance. The disubstituted oligopeptides were less efficient competitors than the mono-substituted oligopeptides.

Binding of Heparan, Chondroitin, and Dermatan Sulfate to rA Homodimers. Soluble LMW-heparin completely inhibited the binding of dimeric rA_{125} to immobilized LMW-heparin at SPR analysis (Figure 7), suggesting that the biotinylation did not alter the binding sites for PDGF. Furthermore, the complete inhibition of binding by soluble LMW-heparin confirmed that the binding of dimeric rA_{125} to the immobilized LMW-heparin was specific. The IC_{50} for LMW-heparin in solution was approximately 200 nM (0.7 μg/mL), closely corresponding to the overall K_D calculated from the Hill plots (Table 3). Three species of GAGs (HS, DS, and CS) almost completely inhibited the binding between the dimeric rA_{125} and immobilized LMW-heparin. According to our results, HS was as potent as LMW-heparin (IC_{50} approximately 0.7 μg/mL), and more efficient than DS and CS (IC_{50} approximately 4 μg/mL).

DISCUSSION

The present results confirm and extend the conclusions from previous studies that binding of the long PDGF-A homodimer to GAGs is due to its basic amino acid carboxyl-terminal extension (Fager et al., 1992b; Raines & Ross, 1992; Andersson et al., 1994; Bondjers et al., 1989; Khachigian & Chesterman, 1994; Khachigian et al., 1992; Östman et al.,

Table 4: Alignment of Heparin-Binding Basic and Polar Amino Acid Residues in the Carboxyl-Terminus of the Long PDGF A-Chain Isoform with Heparin-Binding Motifs of Other Proteins

PDGF long A-chain	bFGF[a]	aFGF[b]	apo B-100[b]
Gly^{108}	Ala^{117}	Gly^{110}	Arg^{3359}
Arg^{109}	Leu^{118}	Leu^{111}	Leu^{3360}
Pro^{110}	Lys^{119}	Lys^{112}	Thr^{3361}
Arg^{111}	**Arg^{120}**	**Lys^{113}**	**Arg^{3362}**
Glu^{112}	Thr^{121}	Asn^{114}	Lys^{3363}
Ser^{113}	Gly^{122}	Gly^{115}	Arg^{3364}
Gly^{114}	Gln^{123}	Arg^{116}	Gly^{3365}
Lys^{115}	Tyr^{124}	Ser^{117}	Leu^{3366}
Lys^{116}	**Lys^{125}**	**Lys^{118}**	**Lys^{3367}**
Arg^{117}	Leu^{126}	Leu^{119}	Leu^{3368}
Lys^{118}	Gly^{127}	Gly^{120}	Ala^{3369}
Arg^{119}	Ser^{128}	Pro^{121}	Thr^{3370}
Lys^{120}	Lys^{129}	Arg^{122}	Ala^{3371}
Arg^{121}	Thr^{130}	Thr^{123}	Leu^{3372}
Leu^{122}	Gly^{131}	His^{124}	Ser^{3373}
Lys^{123}	Pro^{132}	Phe^{125}	Leu^{3374}
Pro^{124}	Gly^{133}	Gly^{126}	Ser^{3375}
Thr^{125}	**Gln^{134}**	**Gln^{127}**	**Asn^{3376}**
COOH	COOH	COOH	Lys^{3370} *

[a] The known motif of bFGF (Thompson et al., 1994). [b] Tentative sequences of apo B-100 and aFGF with commonly positioned types of amino acids marked with bold letters have been displayed for comparison.

1991). To our knowledge, this is the first study to show directly a specific binding between PDGF and heparin, selected as a model GAG, and to elucidate the mechanisms of these interactions *in vitro*. Our results allowed several predictions concerning the interactions between dimeric rA_{125} and heparin.

In SPR analyses, dimeric rA_{109} bound only weakly at high concentrations, while dimeric rA_{125} showed a complex high affinity binding that was completely inhibited either by LMW-heparin or the carboxyl-terminal-derived oligopeptide. This clearly demonstrated the importance of the exon 6-derived basic amino acid extension of the long splice variant of PDGF A and also the specificity of the interaction. The interaction of heparin with the long homodimer shows a positive cooperativity involving hydrophobic forces and seems to be an entropy-driven, endothermic process (Ross & Subramanian, 1981). The kinetic and thermodynamic results supported the concept of an allosteric binding mechanism for dimeric rA_{125}, according to the general model of Monod−Wyman−Changeux (Monod et al., 1965). Thus, dimeric rA_{125} contains equivalent binding sites on each monomer. Upon low affinity binding of heparin to one of these sites, the dimeric rA_{125} undergoes a conformational change inducing high affinity binding of heparin to both sites. The hyperbolic concentration dependency for dimeric rA_{125} and the calculated equilibrium between the high and low binding conformers ($K_2 = 42$, see Results) confirmed the proposed mechanism of interaction. A similar mechanism has been suggested for antithrombin III (AT-III) (Rosenberg, 1985; Jackson et al., 1991). It has also been proposed that the interaction of an extracellular matrix protein, fibronectin, with GAGs modifies its conformation and may have functional consequences with respect to the matrix-driven translocation of cells (Newman et al., 1985, 1987; Yamada et al., 1980).

The analysis of SPR results showed that the actual affinity constant for dimeric rA_{125} was 1.7×10^8 M^{-1}. Our SPR analysis of binding of aFGF to heparin showed an affinity constant of 2×10^6 M^{-1}. This was similar to the previously reported affinity constant of $(7-20) \times 10^6$ M^{-1} (Mach et al., 1993). Consequently, dimeric rA_{125} binds with higher affinity to LMW-heparin than aFGF. Furthermore, the investigation of binding characteristics of monomeric rA_{125}, dimeric rA_{109}, and PDGF-AB suggests that the presence of basic carboxyl-terminals in both monomers is a prerequisite for positive cooperativity and the high binding capacity to LMW-heparin observed in the case of dimeric rA_{125}. The slightly lower K_D of PDGF-AB (0.10 μM) compared to the overall K_D of dimeric rA_{125} (0.50 μM at 26 °C) may suggest the additional sites in the B-chain contributing to the binding. The Hill number of 1 suggests a lack of cooperativity for the heterodimer.

Andersson et al. (1994) suggested that the number of positive amino acids in the carboxyl-terminal extension of the long PDGF A-chain, rather than specific interactions, were of importance for the retention of PDGF on cells or extracellular matrix components. Using competition experiments, we wanted to evaluate directly the contribution of different amino acid residues in the basic carboxyl-terminal extension of dimeric rA_{125} to heparin binding. Monomeric full-length mutants cannot be differentiated from dimeric rA_{125} in SPR and, consequently, they could not be used in competition experiments. Therefore, we used synthetic oligopeptides instead. Carboxyl-terminal-derived oligopeptide (Oligo-RKT) displaced dimeric rA_{125} in SPR analysis with an IC_{50} (2 μM) closely comparable to the dissociation constant of monomeric rA_{125} (6.2 μM) in direct binding experiments. This supports the relevance of using oligopeptides. Our results from displacement experiments, using oligopeptides containing different amino acid substitutions, demonstrate that interaction between dimeric rA_{125} and LMW-heparin depends mainly on three critical amino acids, Arg^{111}, Lys^{116}, and Thr^{125}, in the basic extension and that substitution of these amino acids for alanine abolishes the binding to heparin. Thus, although electrostatic interactions (Arg^{111}, Lys^{116}) are important, the avidity of the interaction may seem to depend more on the (hydrophobic) interaction at Thr^{125}.

Recently, three defined amino acids in the basic sequence of bFGF were reported as essential for the interaction with heparin, the basic residues Arg^{120} and Lys^{125} and the polar residue Gln^{134} (Thompson et al., 1994). These results were further confirmed in crystallographic studies of heparin-derived tetra- and hexasaccharides complexed with bFGF (Faham et al., 1996). These three critical amino acids contained in the basic part of the bFGF sequence have the same character and spatial distribution as the critical amino acids in the carboxyl-terminal extension of dimeric rA_{125}.

In spite of the three residues mentioned above, Asn^{27} was also regarded as important for binding of bFGF to heparin. Although we cannot rule out the possibility, that other amino acids within the PDGF A-chain may contribute to binding, our results with rA_{109} indicate that major independent high affinity binding sites are not present within the sequence common to both isoforms.

Comparison of amino acid sequences of other heparin-binding peptides occurring in the arterial wall shows that similar motifs can be found in aFGF (Lys^{113}, Lys^{118}, and Gln^{127}) and in apoB-100 (Arg^{3362}, Lys^{3367}, and Asp^{3376}). These amino acids are contained in motifs known to bind with high

affinity to heparin (Fager et al., 1995; Mach et al., 1993; Burgess et al., 1990; Harper & Lobb, 1988; Sudhalter et al., 1989; Camejo et al., 1988). In fact, not many more matching alignments of basic and polar amino acid residues were common to these peptide sequences. Our results with the modified PDGF-derived peptides confirmed the relevance of the selection procedure, at least as far as dimeric rA_{125} was concerned.

Standard heparin and LMW-heparin inhibited the DNA synthesis in hASMC *in vitro*. However, heparin, used as a model GAG in our experiments, is exclusively a product of mast cells and is not present in concentrations allowing significant binding of PDGF in tissues, including the arterial wall. We could show previously (Fager et al., 1995) that hASMC *in vitro* synthesized HS, DS, and CS. HS was a dominating side chain among the cell-associated proteoglycans (PGs) and CS among the secreted proteoglycans. We could also show that HS, DS, and CS bound to the PDGF-derived oligopeptide with affinities similar to that of heparin. When evaluating the interaction between the dimeric rA_{125} and GAG species, we have now shown by SPR analyses that all three GAG species inhibit the binding between dimeric rA_{125} and LMW-heparin. According to our displacement experiments, HS was as efficient as LMW-heparin and more efficient than DS and CS. Heparin and HS are structurally similar and they bind and inhibit PDGF with similar efficiency, presumably by similar mechanisms. Regarding the structural requirements of PDGF binding to CS and DS further investigations are necessary.

Commercial GAGs isolated from different sources may differ from corresponding species of the human arterial wall. According to preliminary results from ongoing collaborative research, the hASMC-derived HS behaves similarly to LMW-heparin when binding the dimeric rA-isomers.[2]

The biological implication of our observations needs corroboration in *in vivo* studies. However, it is conceivable that PDGF competes with other GAG-binding molecules for binding sites on GAG side chains of PGs in the arterial wall. It has been proposed that proteins such as PDGF, apo B-100 (Fager et al., 1995), or FGF (Khachigian & Chesterman, 1994) might compete with each other for binding sites on the arterial wall PGs. It may be that the long PDGF-A homodimer would be liable to accumulate, locally bound to and reversibly inactivated by extracellular GAGs and PGs at the site of release, while the short A-chain homodimer would rather disappear from this site as also suggested by others (Raines & Ross, 1992; Andersson et al., 1994; LaRochelle et al., 1991). The accumulation of long A-chain homodimer to GAGs can be further increased by cytokine regulation of the splicing phenomenon (Zhao et al., 1995). An ensuing continuous release of the long PDGF isoform from PG, due to displacement by for instance LDL, FGF, proteolytic enzymes, or endoglycosidases, could stimulate hASMC to proliferation long after the initial arterial injury. Eventually, this may lead to occlusion of the artery. In contrast to PDGF, the FGFs, which may bind to the same binding sites on GAGs, would become activated and protected from proteolytic degradation (Baird & Walicke, 1989). This may suggest that FGF is an early mitogen for ASMC after experimental injury and that PDGF is important later to maintain ASMC proliferation.

[2] Feyzi at al., unpublished observations.

ADDED IN PROOF

In an ongoing study with mutated rA dimers and monomers, the results from SPR analyses suggest that binding and conformational change is accompanied by the binding of two rA dimers to each LMW-heparin molecule.

ACKNOWLEDGMENT

We thank Anne-Li Karlsson and Helena Lindmark for synthesis of oligonucleotides, and Patrik Sundh for synthesis of oligopeptides. We also thank Gudrun Andersson for amino acid analysis of the total hydrolysates of the PDGF peptides.

REFERENCES

Andersson, M., Östman, A., Westermark, B., & Heldin, C.-H. (1994) *J. Biol. Chem. 269*, 926−930.
Baird, A., & Walicke, P. A. (1989) *Br. Med. Bull. 45*, 438−452.
Bobik, A., & Campbell, J. H. (1993) *Pharmacol. Rev. 45*, 1−42.
Bondjers, G., Camejo, G., Fager, G., Olofsson, S.-O., & Wiklund, O. (1989) in *Hypertension and Atherosclerosis. Pathophysiology, Primary and Secondary Prevention* (Dal Palú, C., & Ross, R., Eds.) pp 75−86, Excerpta Medica, Amsterdam, Hong Kong, Manilla, Princeton, Sidney, and Tokyo.
Burgess, W. H., Shaheen, A. M., Ravera, M., Jaye, M., Donohue, P. J., & Winkles, J. A. (1990) *J. Cell. Biol. 111*, 2129−2138.
Camejo, G., Olofsson, S.-O., Lopz, F., Carlsson, P., & Bondjers, G. (1988) *Arteriosclerosis 8*, 368−377.
Elias, P., Gustafsson, C. M., & Hammarsten, O. (1990) *J. Biol. Chem. 265*, 17167−17173.
Fager, G. (1995) *Circ. Res.* 77, 645−650.
Fager, G., Hansson, G. K., Ottosson, P., Dahllöf, B., & Bondjers, G. (1988) *Exp. Cell Res. 176*, 319−335.
Fager, G., Hansson, G. K., Gown, A. M., Larsson, D. M., Skalli, O., & Bondjers, G. (1989) *In Vitro Cell Dev. Biol. 25*, 511−520.
Fager, G., Camejo, G., & Bondjers, G. (1992a) *In Vitro Cell. Dev. Biol. 28A*, 168−175.
Fager, G., Camejo, G., Olsson, U., Östergren-Lundèn, G., & Bondjers, G. (1992b) *In Vitro Cell. Dev. Biol. 28A*, 176−180.
Fager, G., Camejo, G., Olsson, U., Östergren-Linden, G., Lustig, F., & Bondjers, G. (1995) *J. Cell. Physiol. 163*, 380−392.
Faham, S., Hileman, R. E., Fromm, J. R., Linhardt, R. J., & Rees, D. C. (1996) *Science 271*, 1116−1120.
Harper, J. W., & Lobb, R. R. (1988) *Biochemistry 27*, 671−678.
Hart, C.-E., Bailey, M., Curtis, D. A., Osborn, S., Raines, E., Ross, R., & Forstrom, J. W. (1990) *Biochemistry 29*, 166−172.
Heldin, C.-H., Johnsson, A., Wennegren, S., Wernstedt, C., Betsholtz, C., & Westermark, B. (1986) *Nature 319*, 511−514.
Hoebeke, J, Engelborghs, Y., Chamat, S., & Strosberg, A. D. (1987) *Mol. Immunol. 24*, 621−629.
Hoppe, J., Weich, H. A., & Eichner, W. (1989) *Biochemistry 28*, 2956−2960.
Jackson, R. L., Busch, S. J., & Cardin, A. D. (1991) *Physiol. Rev. 71*, 481−539.
Khachigian, L. M., & Chesterman, C. N. (1992) *J. Biol.Chem. 267*, 7478−7482.
Khachigian, L. M., & Chesterman, C. N. (1994) *Peptides 15*, 133−137.
Khachigian, L. M., Owensby, D. A., & Chesterman, C. N. (1992) *J. Biol. Chem. 267*, 1660−1666.
LaRochelle, W. J, May-Siroff, M., Robbins, K. C., & Aaronson, S. A. (1991) *Genes Dev. 5*, 1191−1199.
Lindner, V., & Reidy, M. A. (1991) *Proc. Natl. Acad. Sci. U.S.A. 88*, 3739−3743.
Mach, H., Volkin, D. B., Burke, C. J., Middaugh, C. R., Linhardt, R. J., Fromm, J. R., & Loganathan, D. (1993) *Biochemistry 32*, 5480−5489.

Maher, D. W., Lee, B. A., & Donoghue, D. J. (1989) *Mol. Cell. Biol. 9*, 2251−2253.
Monod, J., Wyman, J., & Changeux, J.-P. (1965) *J. Mol. Biol. 12*, 88−118.
Newman, S. A., Frenz, D. A., Tomasek, J. J., & Rabuzzi, D. D. (1985) *Science (Washington D.C.) 228*, 885−889.
Newman, S. A., Frenz, D. A., Hasegawa, E., & Akiyama, S. K. (1987) *Proc. Natl. Acad. Sci. U.S.A. 84*, 4791−4795.
Östman, A., Andersson, M., Betsholtz, C., Westermark, B., & Heldin, C. H. (1991) *Cell. Regul. 2*, 503−512.
Raines, E. W., & Ross, R. (1992) *J. Cell Biol. 116*, 533−543.
Rosenberg, R. D. (1985) *Fed. Proc. 44*, 404−409.
Ross, P. D., & Subramanian, S. (1981) *Biochemistry 20*, 3096−3102.
Ross, R. (1981) *Arteriosclerosis 1*, 293−311.
Ross, R., Masuda, J., & Raines, E. (1990) *Ann. N.Y. Acad. Sci. 598*, 102−111.
Schwartz, S. M., Campbell, G. R., & Campbell, J. H. (1986) *Circ. Res. 58*, 427−444.
Sudhalter, J., Folkman, J., Svahn, C. M., Bergendahl, K., & D'Amore, P. A. (1989) *J. Biol. Chem. 264*, 6892−6897.
Thompson, L. D., Pantoliano, M. W., & Springer, B. A. (1994) *Biochemistry 33*, 3831−3840.
Thyberg, J., Hedin, U., Sjölund, M., Palmberg, L., & Bottger, B. A. (1990) *Arteriosclerosis 10*, 966−990.
Velge-Roussel, F., Breton, P., Lescure, F., Guillon, X., Bout, D., & Hoebeke, J. (1995) *J. Immunol. Methods 183*, 141−148.
Yamada, K. M., Kennedy, D. W., Kimata, K., & Pratt, R. M. (1980) *J. Biol. Chem. 255*, 6055−6063.
Zhao, X.-M., Frist, W., Yeoh, T.-K., & Miller, G. G. (1995) *Transplantation 59*, 605−611.

BI960118L